Multifunctional control of single-phase transformerless PV inverter connected to a distribution network

Monirul Islam[1], Mithulananthan Nadarajah[1], and Jahangir Hossain[2]
[1]Power and Energy System group, School of ITEE, University of Queensland, Brisbane, Australia
[2]Department of Engineering, Macquarie University, NSW-2109, Australia
mdmonirul.islam@uq.edu.au, mithulan@itee.uq.edu.au, jahangir.hossain@mq.edu.au

***Abstract*—Recently transformerless grid-tied photovoltaic (PV) inverters are getting popular in order to address several concerns; for example, poor efficiency, large size, and heavy weight compared to those with traditional inverter topologies. However, according to the several recently updated grid codes, the grid-tied PV inverter are required to provide full range of services such as maximum power injection, grid voltage regulation (VR), and fault ride through (FRT). In this paper, the performance of a transformerless PV system with a new droop based controller connected to the low voltage distribution system under different operating condition is investigated. In order to provide full-range of grid supporting services, three operation modes are proposed. A detail description of the transformerless PV inverter, droop based controller, and the control strategy are provided. The theoretical analysis is verified using nonlinear simulations in MATLAB/Simulink software environment. The results show that the presented system is capable of injecting maximum power when participate in the grid voltage regulation, and also can enhance fault ride through capability.**

***Index Terms*—Transformerless converter, droop control, fault ride through capability, leakage current, multifunction-control.**

I. Introduction

There has been a massive increase in the total amount of PV installations all over the world during the last decade and most of them are grid-connected [1]. It is mentioned in [2] that the PV installation has reached the 100GW milestone at the end of 2012 which extended to 227.1GW by the end of 2015 as shown in Fig. 1. However, the increasing penetration of PV power into the electric network creates a threat for secure and reliable operation of power system. An unexpected switching of all grid connected PV systems to an unintentional islanding operation could create severe grid problems.

Voltage instability is one of the important aspects of security in power system particularly in high PV penetrated low voltage distribution network [3, 4]. Mostly, the PV system connected to the distribution network does not participate to regulate the voltage. Consequently, the PV inverter operates at unity power factor to maximize the injected real power [5-7]. However, in order to ensure the reliable operation of power system, a number of grid codes, especially in European countries have been updated to regulate the integration of PV system into the distribution network [8-14]. In the German grid code VDE-AR-N 4105, the grid-tied PV inverter of

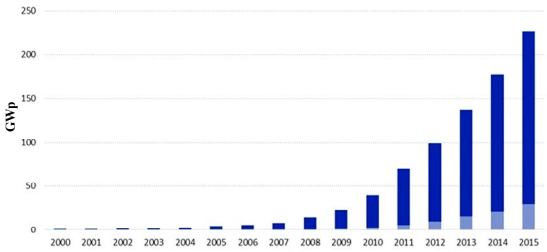

Fig 1. Evaluation of PV installation.

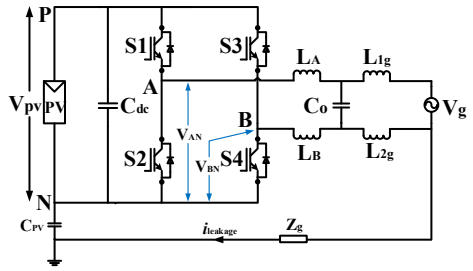

Fig 2. Single-phase transformerless FB inverter for grid-tied PV system.

power rating higher than 4.6kVA, should attain power factor from 0.9 lagging to 0.9 leading [12]. According to the new Italian grid code, grid voltage FRT capability must be provided by the generation units connected to the low voltage networks [15]. The IEEE standard committee has also amended the IEEE 1547 grid code as the distributed energy sources (DES) are allowed to participate to regulate the grid voltage by means of regulating the real and reactive power output that need to be completed by the mutual agreement of both operators of DES and distribution grid [14]. Therefore, the next generation PV inverter should have the ability of injecting or absorbing reactive power to regulate the voltage as well as ride through capability.

Generally, grid-tied PV inverter consists of an isolation transformer to ensure the galvanic separation between the PV module and the grid. The isolation transformer increases the volume, weight and cost, reduces the efficiency, and makes the whole system bulky [16]. As a result, a number of researches have been conducted to remove the transformer [5-7, 17-19]. Though the transformerless inverters have offered high efficiency, compact size and weight, low cost that makes

Identify applicable sponsor/s here. *(sponsors)*

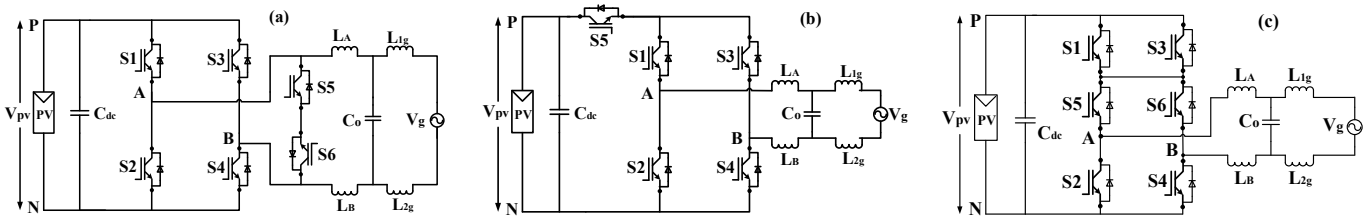

Fig 3. Existing Single-phase transformerless topologies for PV application: (a) HERIC topology (b) H5 topology (c) H6 type topology.

it more attractive; different types of concern like leakage current and dc current injection could be raised by the lack of galvanic isolation between the PV module and the grid. The leakage current flowing through the whole PV system as shown in Fig. 2, can increase the losses, deteriorates the electromagnetic interference, and most significantly, gives rise to a safety issue. It mainly depends on the parasitic capacitance between the PV module and the ground that cannot be neglected, and the fluctuating common mode (CM) voltage that might be generated due to the topology structure and the modulation scheme [20]. The relationship of CM voltage and the leakage current can simply be defined as follows:

$$V_{CM} = \frac{V_{AN} + V_{BN}}{2} \tag{1}$$

$$i_{Leakage} = C_{PV} \frac{dV_{CM}}{dt} \tag{2}$$

where V_{CM} represents CM voltage, V_{AN} and V_{BN} are the controlled voltage source connected to the terminal N, $i_{Leakage}$ is the leakage current, and C_{PV} denotes the parasitic capacitance between the PV module and the ground. It can be seen from equation (1) and (2) that the CM voltage must be kept constant to reduce the leakage current.

In order to meet the leakage current requirement defined by the international standards, a number of researches have been carried out from different countries [5-7, 17-19]. The full-bridge (FB) topology with bipolar modulation presents low leakage current. However, due to the two level output voltage, large output filter is required which increases the losses. Therefore, many transformerless inverters with three-level output voltage have been proposed in the literature by creating modification on the FB topology. Schmidt et al proposed Highly Efficient and Reliable Inverter Concept (HERIC) topology by adding two switches in the ac side of FB inverter as shown in Fig. 3(a) which is also named as full-bridge ac bypass (FB-ACBP) topology [21]. Another transformerless inverter called H5 topology as it is derived from FB topology by adding an extra switch in the dc side has been proposed in [19] which is illustrated in Fig. 3(b). An extension of H5 topology entitled as H6 type topology is presented in [18] which replaces the additional switch with two parallel switches to reduce the stress on the added switch. The switches S5 and S6 of HERIC and H6 type topology, and S5 of H5 topology ensure the decoupling of PV module from the grid during freewheeling period, results constant CM voltage and low leakage current. As transformerless inverter is efficient for grid-tied PV application, it is necessary to explore other issues such as ride through capability, ability to regulate the voltage by injecting or absorbing reactive power which is the main focus of this paper.

In this paper, the performance of a droop based multifunctional control strategy for transformerless grid-tied PV inverters connected to a low voltage distribution system is investigated. Three control modes are considered based on the voltage characteristics of the distribution network. The presented transformerless system is capable to inject or absorb reactive power during the FRT operation. Furthermore, it can support the voltage applied to the local load when operating in Maximum Power Point Tracking (MPPT) mode. Simulation results confirm the performance of the transformerless PV system during three modes of operation. This paper is organized as follows: the droop based control system which includes three controllers for power, voltage and current followed by the proposed control strategy is discussed in Section II. Case studies are carried out to verify the operation modes, and the results and discussions are given in Section III. At last, conclusion and main contribution of the work are highlighted in Section IV.

II. Droop Control of Transformerless Inverter

A. *Review of Droop Based Control Scheme:*

The active and reactive power injected to the grid by the PV inverter which is connected to the grid through a generic impedance as shown in Fig. 4 can be described by the following equation [22]:

$$P = \frac{1}{Z}\left[\left(V_c V_g cos\phi - V_g^2\right) cos\theta + V_c V_g sin\phi sin\theta\right] \tag{3}$$

$$Q = \frac{1}{Z}\left[\left(V_c V_g cos\phi - V_g^2\right) sin\theta - V_c V_g sin\phi cos\theta\right] \tag{4}$$

where V_c and V_g are the inverter and grid voltage respectively, φ is the phase difference between V_c and V_g, P and Q are the active and reactive power. If the phase difference between V_c and V_g is very small, then sinφ = φ and cosφ = 1. Considering X >> R which means R maybe neglected, the equations (3) and (4) becomes:

$$\phi \cong \frac{XP}{V_c V_g} \tag{5}$$

$$V_c - V_g \cong \frac{XQ}{V_g} \tag{6}$$

According to (5) and (6), the power angle depends on the active power while the voltage difference V_c-V_g depends on the reactive power. In other words, the voltage difference could be controlled by regulating reactive power as well as the power angle that controls the frequency by regulating active power. Therefore, the frequency and the inverter output voltage are determined by adjusting the active and reactive power, respectively.

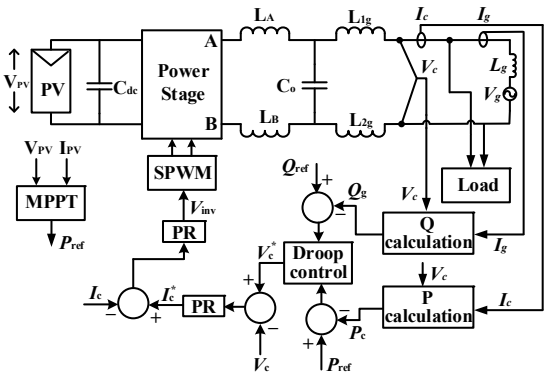

Fig 4. Droop based multifunctional control strategy for transformerless PV system.

B. Droop Based Multifunctional Control Sceme for Transformerless PV Inverter:

According to the prior discussion, the design of next generation grid-tied PV inverter should take into account several factors like efficiency, power quality, fault ride through capability and voltage regulation strategy. By implementing the transformerless inverter, 1-2% efficiency can be improved of the PV system [23]. Therefore, it is important to explore other issues. Fig. 4 shows the overall control structure of the transformerless inverter.

(i) Outer controller design: As shown in Fig. 4, a droop based outer controller is adopted which is responsible for generating the reference of voltage control loop V_{ref}. Typically, the low voltage distribution network shows mainly resistive based impedance. However, the presented transformerless system is connected in parallel to the grid through an inductor L_g as shown in Fig 4. Therefore, in the first step of droop controller design, both X and R is considered for the low voltage network. In that case, if the phase difference between V_c and V_g is very small, (3) and (4) could be modified as follows:

$$P = \frac{1}{Z}\left[\left(V_c V_g - V_g^2\right)cos\theta + V_c V_g \phi sin\theta\right] \tag{7}$$

$$Q = \frac{1}{Z}\left[\left(V_c V_g - V_g^2\right)sin\theta - V_c V_g \phi cos\theta\right] \tag{8}$$

Solving (7) and (8), the control variables can be expressed as follows:

$$V_c - V_g = \frac{Z}{V_g}\left[Pcos\theta + Qsin\theta\right] \tag{9}$$

$$\phi = \frac{Z}{V_c V_g}\left[Psin\theta - Qcos\theta\right] \tag{10}$$

Therefore, the inverter output voltage magnitude and phase angle can be expressed in (11) and (12) to satisfy the active power delivered by the MPPT controller and to compensate the reactive power commanded by the grid [22].

$$V = V^* - G_q(s)\left[(P-P^*)cos\theta + (Q-Q^*)sin\theta\right] \tag{11}$$

$$\phi = \phi^* - G_p(s)\left[(P-P^*)sin\theta - (Q-Q^*)cos\theta\right] \tag{12}$$

where $G_p(s)$ and $G_q(s)$ are the transfer function of the two proportional-integral (PI) based controllers which are proposed to confirm the precise controlling of the active and reactive power as both of them are constant in the steady state. $G_p(s)$ and $G_q(s)$ are defined by the following equations:

$$G_p(s) = K_{pp} + K_{pi} * 1/s \tag{13}$$

$$G_q(s) = K_{qp} + K_{qi} * 1/s \tag{14}$$

where K_{pi} and K_{qi} are the static droop coefficients, while K_{pp} and K_{qp} are known as transient droop terms.

(i) Inner controller design: The voltage and current controllers in the inner control are based on proportional resonant (PR) structure where zero steady state error could be realized by using generalized integrator. Since the quality of the power depends on the current control loop, addition of harmonic compensator (HC) with the PR controller can enhance the tracking performance of the current controller [8]. Therefore, in order to regulate voltage and current, two PR+HC controllers have been adopted. The block diagram of the PR+HC controller for the presented system is depicted in Fig. 5 as well as the transfer functions are given below:

$$G_v(s) = K_{vp} + K_{vi} * \frac{s}{s^2 + \omega_f^2} \tag{15}$$

$$G_i(s) = K_{ip} + K_{ii} * \frac{s}{s^2 + \omega_f^2} \tag{16}$$

$$G_h(s) = \sum_{h=3,5..} K_{i(v)h} * \frac{s}{s^2 + \left(h\omega_f\right)^2} \tag{17}$$

where K_{vp} and K_{ip} are proportional gains, K_{vi} and K_{ii} are resonant gains, ω_f is the fundamental frequency, $K_{i(v)h}$ is the resonant gain at the nth-order harmonic and h is the harmonic order.

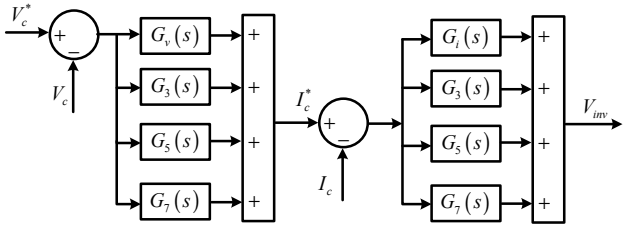

Fig 5. Block diagram of the PR+HC controller.

C. Proposed Control Strategy:

Fig. 6 illustrates the flowchart of the droop based multifunctional control strategy for a single-phase transformerless PV inverter connected to a low voltage distribution network. Based on the grid voltage characteristics, three operation modes (i) Normal MPPT mode, (ii) MPPT with VR mode, (iii) FRT mode, are proposed for the transformerless inverter which are explained briefly in the subsections below.

(i) Normal MPPT mode: When the grid voltage remains between 0.95 to 1.06pu which is the limit of normal operation defined by the standard AS/NZS4777.2 [24], the transformerless inverter operates in normal MPPT mode. During the operation under this mode, the active power reference P_{ref} is calculated according to the MPPT logic while

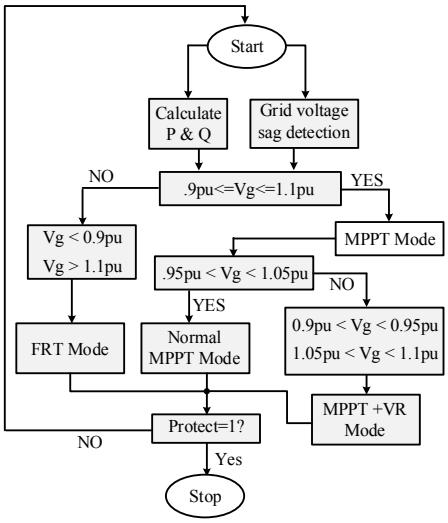

Fig 6. Control flowchart of the droop based multifunctional control strategy for transformerless PV application.

the reactive power reference Q_{ref} is set to be zero. As the system is connected to the grid with local loads, it is likely to be operating in an islanded mode if the local load meets the MPPT.

(ii) MPPT with VR mode: This mode will be activated when the grid voltage turn into 0.9 to 0.95pu or 1.06 to 1.10pu. During the operation period of this mode, the inverter actively injects or absorbs reactive power to keep the load voltage at the desired value, while active power injection follows the MPPT mode. The reactive power reference can be calculated from the required reactive current I_q to compensate the voltage sag as given in (18) [8, 25]:

$$I_q = k\left(1 - V_g\right) I_N \tag{18}$$

where k > 2.

It can be observed that the inverter could be operated over the rated power under this mode when P_{ref} will be equal to the inverter rated power. As a result, the inverter output current may exceed the rated output current which could be one of the causes of inverter failure. Nevertheless, most of the inverter is designed by considering the safety factor. In addition, a time constant t_c that allowed the inverter to be operated during overcurrent, generally has been established in the inverter for high current protection. In this mode, if the transformerless inverter exceeds the rated power and operates for the period of greater than the time constant, it started to follow constant apparent power (CAP) strategy where the inverter output current do not exceed the rated current. In this strategy, the reactive power reference kept as before, while the active power reference is changed from MPPT according to the equation (19) to meet the over current protection.

$$I_{c\max} = \sqrt{I_d^2 + I_q^2} \le I_{rated} \tag{19}$$

where I_{cmax}, I_d, and I_{rated} are the maximum current, active current and rated current of the inverter.

(iii) FRT mode: When the grid voltage surpasses 0.9 or 1.1pu due to the severe fault, the transformerless inverter turns into FRT mode to support the grid as well as maintain the load voltage at the desired value. In this mode, the inverter follows the CAP strategy to avoid over current trip-off. During the operation of this mode, the reactive power reference is calculated according to the reactive current injection requirement defined by the E.ON grid code as given in equation (18) [25]. Like as previous mode, the active power reference is changed from MPPT according to equation (19) to keep the apparent power constant at rated.

III. CASE STUDIES

In order to verify the effectiveness of the multifunctional control strategy for transformerless PV system, several case studies are carried out in the MATLAB/Simulink software environment. The transformerless topology presented in Fig. 3(c) is selected to be verified. The parameters that have been considered for simulation are given in Table I. In this analysis, the PV module is replaced with a dc source, and the parasitic capacitance between the PV module and the ground is emulated with a capacitor of 100nF.

TABLE I
SPECIFICATION OF THE PROTOTYPE

Inverter Parameter	Value
Input Voltage	380VDC
Grid Voltage / Frequency	230V / 50Hz
Switching Frequency	20kHz
dc bus capacitor	1000µF
Filter capacitor	2.2µF
Filter Inductor L_A, L_B / L_{1g}, L_{2g}	1mH / 0.5mH
K_{pp}, K_{pi}, K_{qp}, K_{qi}	.0003, .006, .0005, .0009
K_{ip}, K_{ii}, K_{vp}, K_{vi}	.05, 40, .15, 25

A. Performmance of normal MPPT mode:

The output voltage and current, grid voltage and current, load current, active and reactive power, and leakage current for the transformerless inverter during normal MPPT mode is shown in Fig. 7. It can be seen that the inverter can inject maximum real power into the grid as well as maintain the local load with low leakage current. However, if the local load meets the MPPT, the inverter operates in islanding mode to satisfy the local demand as given in Fig 8. In addition, it can be observed from Fig 9 that if the local load increases more than MPPT capability, the extra load has been supplied by the grid. Furthermore, the root mean square (RMS) value of leakage current flows through the whole system is measured 13mA which is lower than the requirement of the standard VDE-AR-N 4105 during the operation of this mode.

B. Performance of MPPT with VR mode:

In order to verify the MPPT with VR mode, small voltage sag which equals to 0.09pu is created on the grid at 0.6s. Fig. 10 demonstrates that the inverter can inject required reactive power into the grid to restore the voltage. However, it can also be observed from Fig. 11 that the inverter turns into the FRT mode by dropping the active power injection at 1.1 s to avoid unintentional trip-off as the grid voltage sag remains for the period more than the time constant which is set 0.5 s. During the operation under this mode, the transformerless inverter keeps the leakage current below the limit of the standard as shown in Figs 10 and 11. Therefore, the inverter

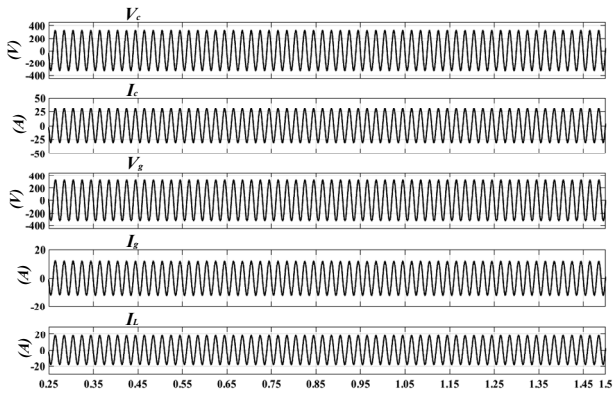

(a)

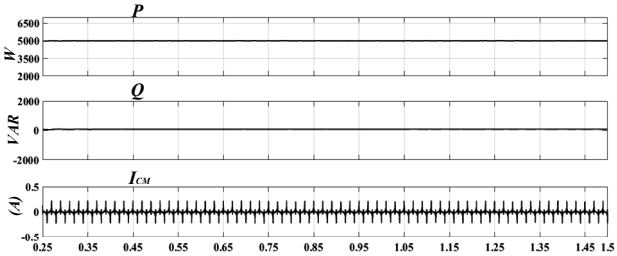

(b)

Fig 7. Steady state operation: (a) output volatge V_c, output current I_c, grid volatge V_g, grid current I_g, and load current I_L (b) real power P, reactive power Q, and leakage current I_{CM}.

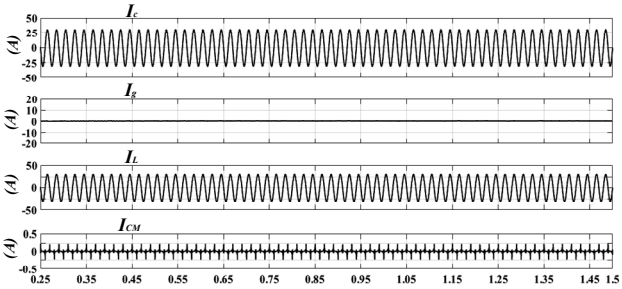

Fig 8. Steady state operation when the local load meets the MPPT.

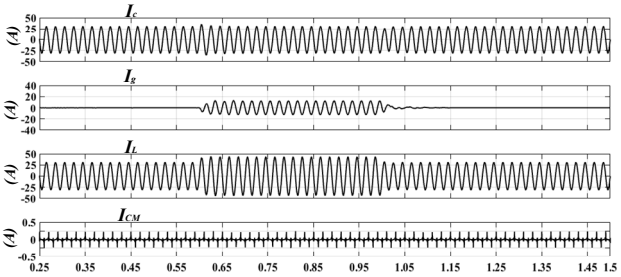

Fig 9. Performance of the transformerless system when the local load suddenly increases than MPPT.

is capable of injecting maximum power during small voltage sag as well as maintain rated power at output to avoid unintentional trip-off if the sag remains.

C. *Performance of FRT mode:*

The performance of the proposed system under FRT mode is confirmed by creating a voltage sag and swell

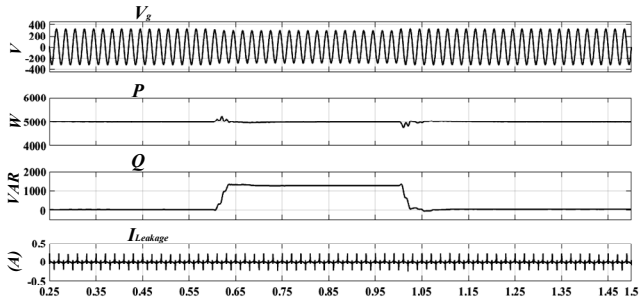

Fig 10. Power flow and leakage current with 0.09pu grid voltage sag.

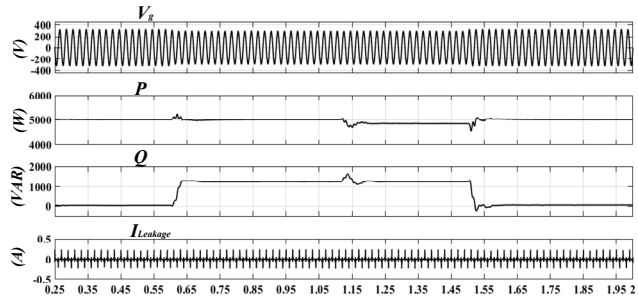

Fig 11. Power flow and leakage current when 0.09pu grid voltage sag remain more than t_c.

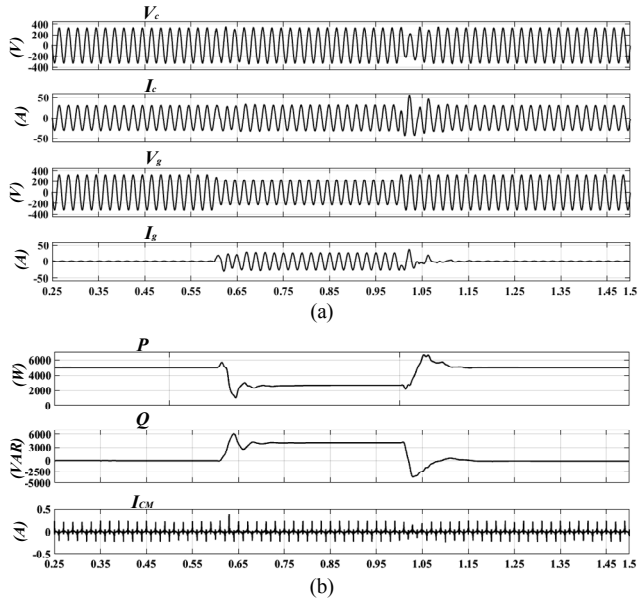

(a)

(b)

Fig 12. Performance of the transformerless PV system with 0.3pu grid voltage sag: (a) output characteristics (b) power flow and leakage current.

which equals to 0.3pu on the grid at 0.6s. The results are shown in Figs 12-13. It can be seen that the transformerless inverter can inject when voltage sag occurs as shown in Fig. 12 or absorb when voltage swell ensured as shown in Fig. 13, reactive power according to the requirement of the grid codes. As shown in Figs. 12(a) and 13(a), a distortion can be noticed during voltage sag or swell which is the results of power calculation delay. However, this distortion has been recovered within very short period. It can also be observed a high peak of leakage current during the transient of voltage sag in Fig. 12(b) which is still below the requirement of the international standard.

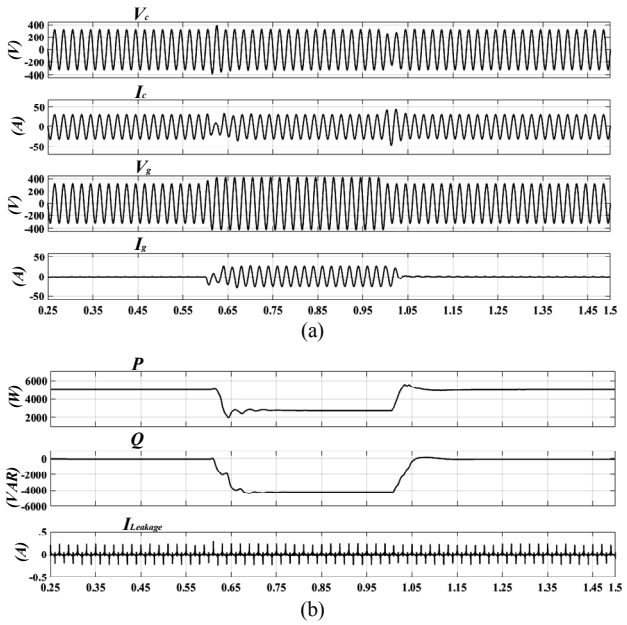

Fig 13. Performance of the transformerless PV system with 0.3pu grid voltage swell: (a) output characteristics (b) power flow and leakage current.

IV. CONCLUSIONS

In this paper, a single phase transformerless grid-tied PV system with droop based control strategy for multifunction objective is examined. In order to realize multifunction with transformerless topology, a control strategy is suggested where three modes are proposed considering different scenarios. It is shown that during normal operation, the transformerless PV system injects only active power to maximize the efficiency; as well as if small voltage sag or swell happens, it can inject or absorb reactive power respectively to restore the voltage. In addition, if severe voltage sag or swell is occurred in the grid due to the unintentional fault, the transformerless system can contribute to compensate the sag or swell which are the requirements of the different international standards. Moreover, during the all operation modes, the leakage current is kept below the requirement which secure it for transformerless PV application. Therefore, it can be concluded that the multifunction features in conjunction with high efficiency can make the transformerless PV system more attractive.

V. REFERENCES

[1] I. PVPS, "Snapshot of global photovoltaic markets 2015," *Report IEA-PVPS T1–29,* 2016.

[2] I. PVPS, "Trends in photovoltaic applications. Survey report of selected IEA countries between 1992 and 2014," *Report IEA-PVPS T1–27,* 2015.

[3] J. Yaghoobi, N. Mithulananthan, and T. K. Saha, "Dynamic voltage stability of distribution system with a high penetration of rooftop PV units," in *2015 IEEE Power & Energy Society General Meeting*, 2015, pp. 1-5.

[4] M. J. Hossain, M. A. Mahmud, H. R. Pota, and N. Mithulananthan, "Design of Non-Interacting Controllers for PV Systems in Distribution Networks," *IEEE Transactions on Power Systems,* vol. 29, pp. 2763-2774, 2014.

[5] J. Baojian, W. Jianhua, and Z. Jianfeng, "High-Efficiency Single-Phase Transformerless PV H6 Inverter With Hybrid Modulation Method," *IEEE Transactions on Industrial Electronics,* vol. 60, pp. 2104-2115, 2013.

[6] M. Islam and S. Mekhilef, "Efficient Transformerless MOSFET Inverter for a Grid-Tied Photovoltaic System," *IEEE Transactions on Power Electronics,* vol. 31, pp. 6305-6316, 2016.

[7] R. Gonzalez, J. Lopez, P. Sanchis, and L. Marroyo, "Transformerless Inverter for Single-Phase Photovoltaic Systems," *IEEE Transactions on Power Electronics,* vol. 22, pp. 693-697, 2007.

[8] Y. Yang, F. Blaabjerg, and H. Wang, "Low-Voltage Ride-Through of Single-Phase Transformerless Photovoltaic Inverters," *IEEE Transactions on Industry Applications,* vol. 50, pp. 1942-1952, 2014.

[9] J. E.-G. Carrasco, J. M. Tena, D. Ugena, J. Alonso-Martinez, D. Santos-Martin, and S. Arnaltes, "Testing Low Voltage Ride Through capabilities of solar inverters," *Electric Power Systems Research,* vol. 96, pp. 111-118, 3// 2013.

[10] E. J. Coster, J. M. A. Myrzik, B. Kruimer, and W. L. Kling, "Integration Issues of Distributed Generation in Distribution Grids," *Proceedings of the IEEE,* vol. 99, pp. 28-39, 2011.

[11] "IEEE Recommended Practice and Requirements for Harmonic Control in Electric Power Systems," *IEEE Std 519-2014 (Revision of IEEE Std 519-1992),* pp. 1-29, 2014.

[12] T. F. Wu, C. L. Kuo, K. H. Sun, and H. C. Hsieh, "Combined Unipolar and Bipolar PWM for Current Distortion Improvement During Power Compensation," *IEEE Transactions onPower Electronics,* vol. 29, pp. 1702-1709, 2014.

[13] M. Islam, S. Mekhilef, and M. Hasan, "Single phase transformerless inverter topologies for grid-tied photovoltaic system: A review," *Renewable and Sustainable Energy Reviews,* vol. 45, pp. 69-86, 2015.

[14] T. Basso, S. Chakraborty, A. Hoke, and M. Coddington, "IEEE 1547 Standards advancing grid modernization," in *Photovoltaic Specialist Conference (PVSC), 2015 IEEE 42nd*, 2015, pp. 1-5.

[15] Y. Yongheng, F. Blaabjerg, and W. Huai, "Low-Voltage Ride-Through of Single-Phase Transformerless Photovoltaic Inverters," *IEEE Transactions on Industry Applications,* vol. 50, pp. 1942-1952, 2014.

[16] Z. Li, S. Kai, X. Yan, and X. Mu, "H6 Transformerless Full-Bridge PV Grid-Tied Inverters," *IEEE Transactions on Power Electronics,* vol. 29, pp. 1229-1238, 2014.

[17] X. Huafeng, X. Shaojun, C. Yang, and H. Ruhai, "An Optimized Transformerless Photovoltaic Grid-Connected Inverter," *IEEE Transactions on Industrial Electronics,* vol. 58, pp. 1887-1895, 2011.

[18] M. Islam and S. Mekhilef, "H6-type transformerless single-phase inverter for grid-tied photovoltaic system," *IET Power Electronics,* vol. 8, pp. 636-644, 2015.

[19] M. Victor, F. Greizer, S. Bremicker, and U. Hübler, "Method of converting a direct current voltage from a source of direct current voltage, more specifically from a photovoltaic source of direct current voltage, into a alternating current voltage," ed: United States Patents, 2008.

[20] X. Huafeng and X. Shaojun, "Leakage Current Analytical Model and Application in Single-Phase Transformerless Photovoltaic Grid-Connected Inverter," *IEEE Transactions on Electromagnetic Compatibility,* vol. 52, pp. 902-913, 2010.

[21] D. Schmidt, D. Siedle, and J. Ketterer, "Inverter for transforming a DC voltage into an AC current or an AC voltage," ed: EP Patent 1,369,985, 2009.

[22] J. C. Vasquez, R. A. Mastromauro, J. M. Guerrero, and M. Liserre, "Voltage support provided by a droop-controlled multifunctional inverter," *IEEE Transactions on Industrial Electronics,* vol. 56, pp. 4510-4519, 2009.

[23] T. Kerekes, R. Teodorescu, P. Rodriguez, G. Vazquez, and E. Aldabas, "A New High-Efficiency Single-Phase Transformerless PV Inverter Topology," *IEEE Transactions on Industrial Electronics,* vol. 58, pp. 184-191, 2011.

[24] J. D. Watson, N. R. Watson, D. Santos-Martin, A. R. Wood, S. Lemon, and A. J. V. Miller, "Impact of solar photovoltaics on the low-voltage distribution network in New Zealand," *IET Generation, Transmission & Distribution,* vol. 10, pp. 1-9, 2016.

[25] Y. Yang, H. Wang, and F. Blaabjerg, "Reactive Power Injection Strategies for Single-Phase Photovoltaic Systems Considering Grid Requirements," *IEEE Transactions on Industry Applications,* vol. 50, pp. 4065-4076, 2014.